

<sup>1</sup> Bayesian inference of prehistoric population dynamics from multiple  
<sup>2</sup> proxies: a case study from the North of the Swiss Alps

<sup>3</sup> Martin Hinz<sup>1,2,\*</sup>      Joe Roe<sup>1</sup>      Julian Laabs<sup>3</sup>      Caroline Heitz<sup>3</sup>      Jan Kolář<sup>4,5</sup>

<sup>4</sup> 30 Mai, 2022

<sup>5</sup> **Abstract**

Robust estimates of population are essential to the study of human–environment relations and socio-ecological dynamics in the past. Population size and density can directly inform reconstructions of prehistoric group size, social organisation, economic constraints, exchange, and political and social institutions. In this pilot study, we present an approach that we believe can be usefully transferred to other regions, as well as refined and extended to greatly advance our understanding of prehistoric demography. Here, we present a Bayesian hierarchical model that uses Poisson regression and state-space representation to produce absolute estimates of past population size and density. Using the area North of the main ridge of the Swiss Alps in prehistoric times (6000–1000 BCE) as a case study, we show that combining multiple proxies (site counts, radiocarbon dates, dendrochronological dates, and landscape openness) produces a more robust reconstruction of population dynamics than any single proxy alone. The model's estimates of the credibility of its prediction, and the relative weight it affords to individual proxies through time, give further insights into the relative reliability of the evidence currently available for paleodemographic research. Our prediction of population development of the case study area accords well with the current understanding in the wider literature, but provides a more precise and higher-resolution estimate that is less sensitive to spurious fluctuations in the proxy data than existing approaches, especially the popular summed probability distribution of radiocarbon dates. The archaeological record provides several potential proxies of human population dynamics, but individually they are inaccurate, biased, and sparse in their spatial and temporal coverage. Similarly, current methods for estimating past population dynamics are often simplistic: they work on limited spatial scales, tend to rely on a single proxy, and are rarely able to infer population size or density in absolute terms. In contemporary demography, it is becoming increasingly common to use Bayesian statistics to estimate population trends and project them into the future. The Bayesian approach is popular because it offers the possibility of combining heterogeneous data, and at the same time quantifying the uncertainty and credibility attached to forecasts. These same characteristics make it well-suited to applications to archaeological data in paleodemographic studies.

<sup>30</sup> <sup>1</sup> Institute of Archaeological Sciences, University of Bern

<sup>31</sup> <sup>2</sup> Oeschger Centre for Climate Change Research, University of Bern

<sup>32</sup> <sup>3</sup> CRC 1266 - Scales of Transformation, University of Kiel

<sup>33</sup> <sup>4</sup> Department of Vegetation Ecology, Institute of Botany of the Czech Academy of Sciences

<sup>34</sup> <sup>5</sup> Institute of Archaeology and Museology, Faculty of Arts, Masaryk University

<sup>35</sup> \* Correspondence: Martin Hinz <martin.hinz@iaw.unibe.ch>

<sup>36</sup> Keywords: Prehistoric demography; Bayesian modelling; Multi-proxy; Settlement dynamics

<sup>37</sup> Highlights: - Bayesian modelling can integrate multiple, heterogeneous population proxies from the archaeological record - Our initial model produces more robust, high-resolution estimates of past population dynamics than previous, single-proxy approaches - We provide absolute estimates of population size and density on the area north of the Swiss Alps in prehistoric times (6000–1000 BCE)

## 41 1. Introduction

42 Prehistorians have long recognised demography as a fundamental force in human cultural evolution (Childe,  
43 1936). Despite decades of interest in the population dynamics of prehistoric societies, concrete estimates  
44 of population size and density before written records remain elusive. Though the archaeological record  
45 provides multiple possible demographic proxies (Müller and Diachenko, 2019), a lack of access to this data  
46 and methodological tools for turning it into quantitative estimates has left the conclusions drawn from it  
47 vague and superficial (Hassan, 1981). As a result, ‘expert estimates’ transferred from ethnographic parallels  
48 have often taken the place of direct inference from archaeological evidence Turchin et al. (2015).

49 Prehistoric demography has experienced a resurgence in interest in recent years (Riede, 2009 and others in  
50 same issue; Shennan, 2000), partly explained by a renewed interest in human–environment relations and  
51 human impact, necessarily requiring an assessment of population size. Kintigh et al. (2014) list human  
52 influence, dominance, population size, and population growth amongst their ‘grand challenges’ for archaeology  
53 in the 21st century.

54 In particular, the ‘dates as data’ technique (Rick, 1987), using the frequency of radiocarbon dates as a proxy  
55 for population dynamics, has been significantly developed in the last decade (e.g. Shennan et al., 2013) and  
56 widely applied to archaeological contexts worldwide (Crema, 2022). This approach has contributed greatly to  
57 our understanding of prehistoric demography, but is not without its critics Carleton and Groucutt (2021).  
58 While the methodology continues to evolve and address these critiques (Crema, 2022), it remains subject  
59 to fundamental problems common to all approaches relying on a single proxy Schmidt et al. (2021). We  
60 believe that these problems cannot be overcome by methodological refinements in this area alone. Instead, a  
61 Bayesian approach offers a robust, quantitative methodology for inferring prehistoric population dynamics  
62 from multiple proxies, including summed radiocarbon dates.

## 63 2. Background

### 64 2.1. Population estimation in prehistory

65 Proxies currently used for the estimation of population size in prehistory (following Müller and Diachenko, 2019)  
66 can roughly be divided into three groups: ethnographic analogies; deductive estimates from ecological/economic  
67 factors; and the interpolation of frequencies of archaeological features (e.g. settlements, structures, individual  
68 finds). Three basic problems are common to all these approaches:

- 69 1. **Reliance on single proxy:** Most investigations use only one source of evidence. Although multi-proxy  
70 approaches exist, the individual proxies only serve to support each other or the main estimator, without  
71 explicitly combining them.
- 72 2. **Uncertainty in measurements:** All archaeological evidence is inherently uncertain which is carried  
73 through to derived measurements. However, in most studies, single curves are presented as estimates,  
74 and the potential error associated is almost never specified.
- 75 3. **Lack of a transfer function:** By ‘transfer function’, we mean something that allows for the proxy data  
76 to be interpreted in terms of actual population size or density. This could be absolute, i.e. a numerical  
77 estimate of population, or relative, i.e. a means of scaling changes in the proxy value to changes in  
78 population. Lack of suitable frameworks and ‘calibration’ data means that this is rarely presented  
79 alongside proxy estimates. In the best cases, there is a qualitative assessment of the informative value  
80 of the proxy, not sufficiently accounting for the complex nature of archaeological data.

81 Furthermore, the types of archaeological data commonly used as population proxies share a number of  
82 problematic characteristics, being:

- 83 • **Limited:** We have only incomplete data, and it is usually not very informative.
- 84 • **Unevenly distributed:** For example, although there is a good data on settlement frequencies for  
85 some regions, these regions are very unevenly distributed over time and space.
- 86 • **Noisy:** Frequently individual proxies are strongly influenced by factors unrelated to population, for  
87 example taphonomic conditions or depositional biases.

- 88 • **Unreliable:** Research strategies, research history and varying levels of resources available to researchers  
 89 strongly affect the nature of compiled datasets. Systematic distortions are the rule rather than the  
 90 exception.
- 91 • **Heterogeneous:** All potential proxies have different spatio-temporal scales, granularity, information  
 92 value, scales, and data formats.
- 93 • **Indirect:** We will never have direct data on prehistoric population; only proxy data that is thought to  
 94 be a reasonable substitute. The transfer functions linking the proxy data with the desired quantity  
 95 (population) are unknown.
- 96 • **Contradictory:** When considering several proxies, differences in transfer functions, data quality and  
 97 noisiness inevitably lead to different results.
- 98 Many, if not all, of these problems can be ameliorated through a) the explicit, quantitative integration of  
 99 multiple proxies; and b) the use of a Bayesian approach to take account of and estimate uncertainty.

## 100 2.2. Hierarchical Bayesian demographic models

101 Many of the problems with archaeological population proxies are shared with contemporary demography. In  
 102 response, demographers have increasingly turned to Bayesian methods to estimate and forecast contemporary  
 103 population dynamics. For example, Bryant and Zhang (2018) consider Bayesian data modelling a solution  
 104 to exactly the kind of problems that affect archaeological data. Bayesian approaches are well suited for  
 105 limited, unreliable and noisy data. Various data sources, even contradictory data, can be brought into a  
 106 common framework and used to support one another. These methods also provide a quantitative estimate of  
 107 the likelihood and uncertainty of the model's resulting predictions (or in our case retro-dictions). Bayesian  
 108 approaches are also capable of accounting for spatially and temporally incomplete data: where this data  
 109 is missing, the uncertainty increases, but this does not prevent general modelling and estimation. Finally,  
 110 hierarchically-structured model suites, with sub-models for each individual proxy, can be used to estimate  
 111 transfer functions between them and the value to be modelled, thanks to the interaction of a large number of  
 112 evidence.

113 This modeling technique can thus be used to join different lines of evidence horizontally and vertically and  
 114 combine their results into a overall estimate, including an assessment of their reliability: contradicting data  
 115 lead to a lower overall reliability, while a mutual support to smaller confidence intervals. If there is no  
 116 systematic bias that affects all data sources to the same extent, this results in the most reliable estimate  
 117 possible through the most heterogeneous set of data sources.

118 Bayesian radiocarbon calibration is a similar, well-established application in archaeology, where radiometric  
 119 uncertainty is modelled based on prior stratigraphic information. More recently, archaeologists have also  
 120 used Bayesian modelling techniques for testing hypotheses relating to demographic models based on  $^{14}\text{C}$  data  
 121 (e.g. Crema and Shoda, 2021). This approach differs from the one presented here in that, in these analyses,  
 122 deductive models are generated and their plausibility is tested on the basis of  $^{14}\text{C}$  data only. This is a clear  
 123 step forward to a model-based, scientific analysis. However, the use of only one proxy, exclusively for testing  
 124 hypotheses developed independently, creates problems comparable to those of the inductive approaches used  
 125 so far: lacking a combination with other indicators, one is limited to the problems and conditions of sum  
 126 calibration. Furthermore, this approach loses significant potential information that would be gained by a  
 127 direct evaluation of time series.

128 We attempt to make Bayesian hierarchical techniques usable for archaeological reconstructions. We want to  
 129 show, in a reproducible and practical form using a case study, how Bayesian methods can make a decisive  
 130 contribution to a better assessment of population development, crucial for the reconstruction of the human  
 131 past, even in for periods for which we only have very patchy, noisy and unreliable data.

## 132 2.3. The Bayesian approach

133 Bayesian statistics relies on the premise that there is always some prior assumption, even if very rough,  
 134 about the probability of an event. This assumption is adjusted by observing data, by checking how credible  
 135 these priors are (likelihood, see also Bryant and Zhang, 2018, p. 66). This is Bayesian updating (cf. also

136 Kruschke, 2015, especially 15–25), resulting in the posterior probability distribution, which represents not a  
137 point prediction. Small amounts of data lead to a broad distribution not strongly localised and restricted.  
138 Thus, we simultaneously obtained a result and an estimate the credibility interval, given the data.

139 This Bayesian learning is iterative and sequential, so that the result of one Bayesian inference can form the  
140 prior of another (Kruschke, 2015, p. 17). This allows different information to be combined (Bryant and  
141 Zhang, 2018, pp. 219–224), as it has long been exploited by archaeology in using stratigraphic information to  
142 make radiometric dating more accurate (Ramsey, 1995).

143 This also makes a hierarchical formulation of problem domains possible. Parameters that are necessary for an  
144 estimation, such as the relationship of population density to the deforestation signal in pollen data, need  
145 not be specified explicitly, but can be given by probability distributions and then estimated in the model  
146 itself (Bryant and Zhang, 2018, p. 186). The more data available, the more degrees of freedom can be  
147 estimated with a reasonable width of credibility intervals (Kruschke, 2015, p. 112). For the estimation of  
148 these parameters, submodels have to be created describing the relationship of the data to the characteristics  
149 of the parameter (Kruschke, 2015, pp. 221–222).

### 150 3. Materials: population proxy data

151 Our case study area north of the Swiss Alps (Figure 1) covers about one third of Switzerland’s territory and  
152 comprises the partly flat, but largely hilly area between the Jura Mountains and the Alps. It is favourable  
153 for settlement and agriculture; the Swiss Plateau between Lake Zurich and Lake Geneva is by far the most  
154 densely populated region of the Switzerland today. This serves as our core region of interest because it  
155 is here that archaeological data is most abundant and accessible. The region has a very diverse natural  
156 landscape: shaped by glaciers during the ice ages, the many lakes and bogs provide excellent preservation  
157 conditions for the numerous Neolithic and Bronze Age lakeside settlements, and a rich source for vegetation  
158 reconstructions by means of pollen analyses. Thanks to the very active and efficient archaeological research  
159 and heritage management there is an abundance of archaeological information, including known sites as well  
160 as dendrochronological and  $^{14}\text{C}$  data.

161 Our case study targets the period between 6000–1000 BCE. The lower limit of this time window was chosen  
162 to avoid the so-called ‘Hallstatt plateau’ in the Northern Hemisphere radiocarbon calibration curve, which  
163 causes difficulties for the  $^{14}\text{C}$  proxy. The upper limit coincides with post-glacial changes in pollen spectra,  
164 before which the openness indicator is highly unlikely to reflect human influence.

165 A large number of different proxies can be integrated into a model of this type, provided that these observations  
166 a) can be understood as dependent on the population density in the past, and b) a model-like description  
167 of this dependence can be created. Table 1 provides a non-exhaustive list. For our case study, we used a  
168 landscape openness indicator; an aoristic sum of typological dated sites; a sum calibration; and frequency  
169 data for dendro-dated lakeshore settlements in the Three Lakes region (western Swiss Plateau).

Table 1: A incomplete list of possible observation that can be linked  
to population developments in the past. Proxies used in this study  
are highlighted.

Proxies
Expert estimates
Ethnographic Analogies
Carrying Capacity
Economic modelling
Extrapolation of buried individuals
Burial anthropology
Settlement data, number of houses
Settlement data, settlement size
<b>Aoristic analysis</b>

Proxies
<b>Dendro dates</b>
Amount of archaeological objects
<b>Radiocarbon sum calibration</b>
Estimates based on specific object types
<b>Human impact from pollen or colluvial data</b>
aDNA based estimates
...

### 170 3.1. Dendro-dated lakeshore settlements

171 From the Neolithic onwards, known settlement areas in Switzerland concentrate along its rivers and lakes  
 172 (Christian Lüthi, 2009). Thus, our working region offers excellent data for demographic estimation, but  
 173 poses very specific problems for such an undertaking. We have high-resolution information on the temporal  
 174 sequence of individual lakeside settlements by means of dendro data. In these cases,  $^{14}\text{C}$  data are not as  
 175 abundant simply because they are inferior to dendro dating.

176 The dataset we use for the number of dendro-dated wetland settlements in the Three Lakes region was  
 177 collected by Julian Laabs for his PhD thesis (Laabs, 2019). The time series used here runs from 3900 to 800  
 178 BCE, and contains the number of chronologically registered fell phases at individual settlements.

### 179 3.2. Summed radiocarbon

180 The dataset for the  $^{14}\text{C}$  sum calibration primarily consists of data from the XRONOS database (<https://xronos.ch>), supplemented by dates from the unpublished PhD thesis of Julian Laabs (Laabs, 2019) and the  
 181 data collection of Martínez-Grau et al. (2021). It contains a total of 1135 single  $^{14}\text{C}$  data from 246 sites  
 182 (see Figure 2). The dates in the dataset range in  $^{14}\text{C}$  years from 10730 to 235 uncal BP. This time window  
 183 extends beyond the study horizon in order to minimise boundary effects.

184 We binned the data at site levels to obtain a temporally dispersed count and thus an expected value of  
 185 contemporaneous  $^{14}\text{C}$  dated sites. For the creation of the sum calibration, the corresponding functions of the  
 186 R package rcarbon (Crema and Bevan, 2021) were used with their default settings.

### 188 3.3. Aoristic sum

189 We include relative dating information obtained from the heritage authorities of the Swiss cantons (Figure 3).  
 190 These are primarily derived from scattered surface finds, often with a low dating accuracy (only in the range  
 191 of archaeological periods), incorporated into our model as a typologically-dated, aorist time series. However,  
 192 it is not dependent radiocarbon dating and thus it avoids the methodological issues of sum calibration. Data  
 193 from 4321 sites were included in the aoristic sum.

### 194 3.4. Landscape openness

195 Natural conditions in the Swiss lakes enable not only highly precise dating of archaeological sites, but also  
 196 a very dense network of pollen analysis. We make use of this by generating a supra-regional openness  
 197 indicator for the vegetation from the pollen data (Figure 5). This proxy has the specific advantage that it is  
 198 not dependent on archaeological preservation conditions, making it particularly valuable for compensating  
 199 systematic distortions that result from archaeological taphonomy and period-specific settlement patterns.

200 We assume that the higher the population density in an area, the greater the human influence on the  
 201 natural environment Lechterbeck et al. (2014). Evidence of deforestation can therefore provide indications of  
 202 population dynamics. The full procedure for deriving this proxy from several different pollen diagrams is  
 203 detailed in a previous publication (Heitz et al., 2021). Here, we use five pollen diagrams from sites mainly in  
 204 the hinterland of the large Alpine lakes.

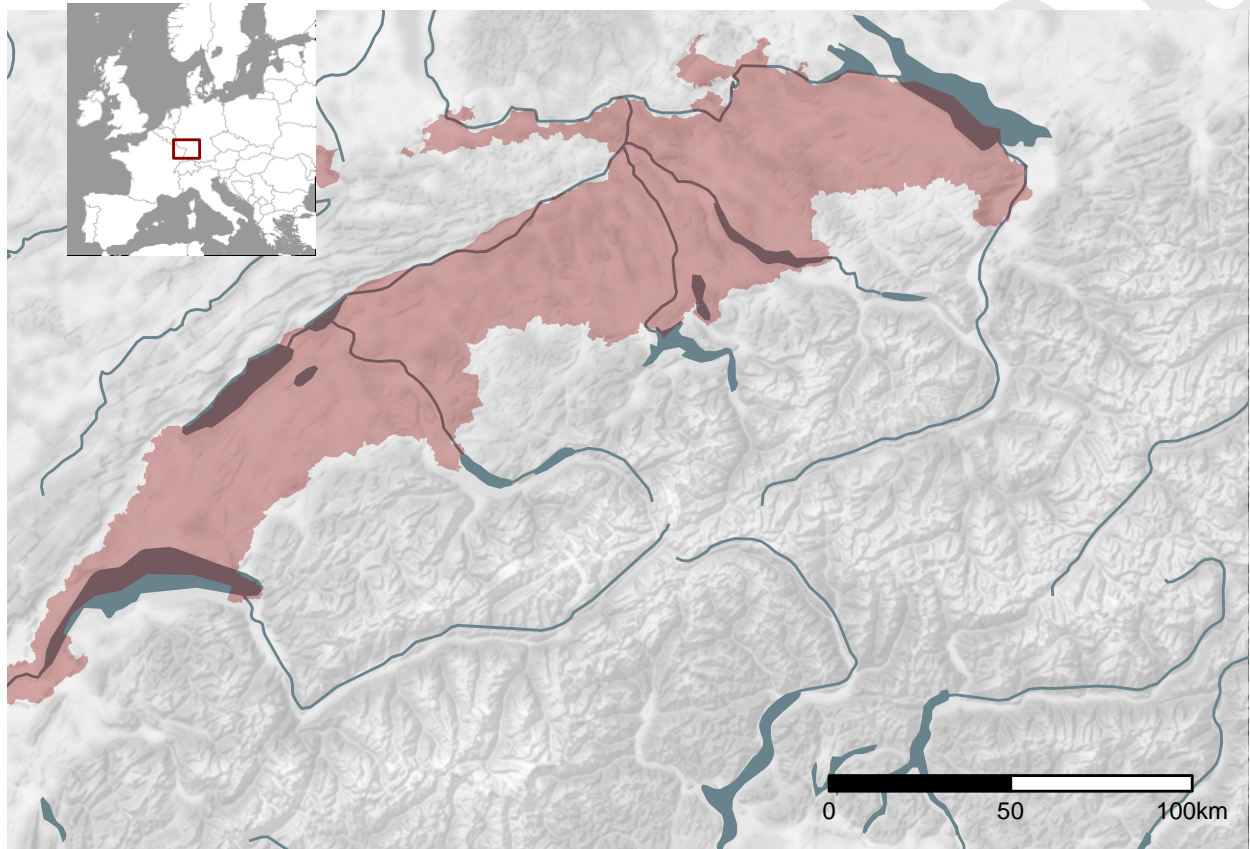


Figure 1: Location and extent of the Swiss Plateau as biogeographical region (based on swisstopo) including additional low altitude areas in the north of Switzerland (regions along the High Rhine between Schaffhausen and Basel).

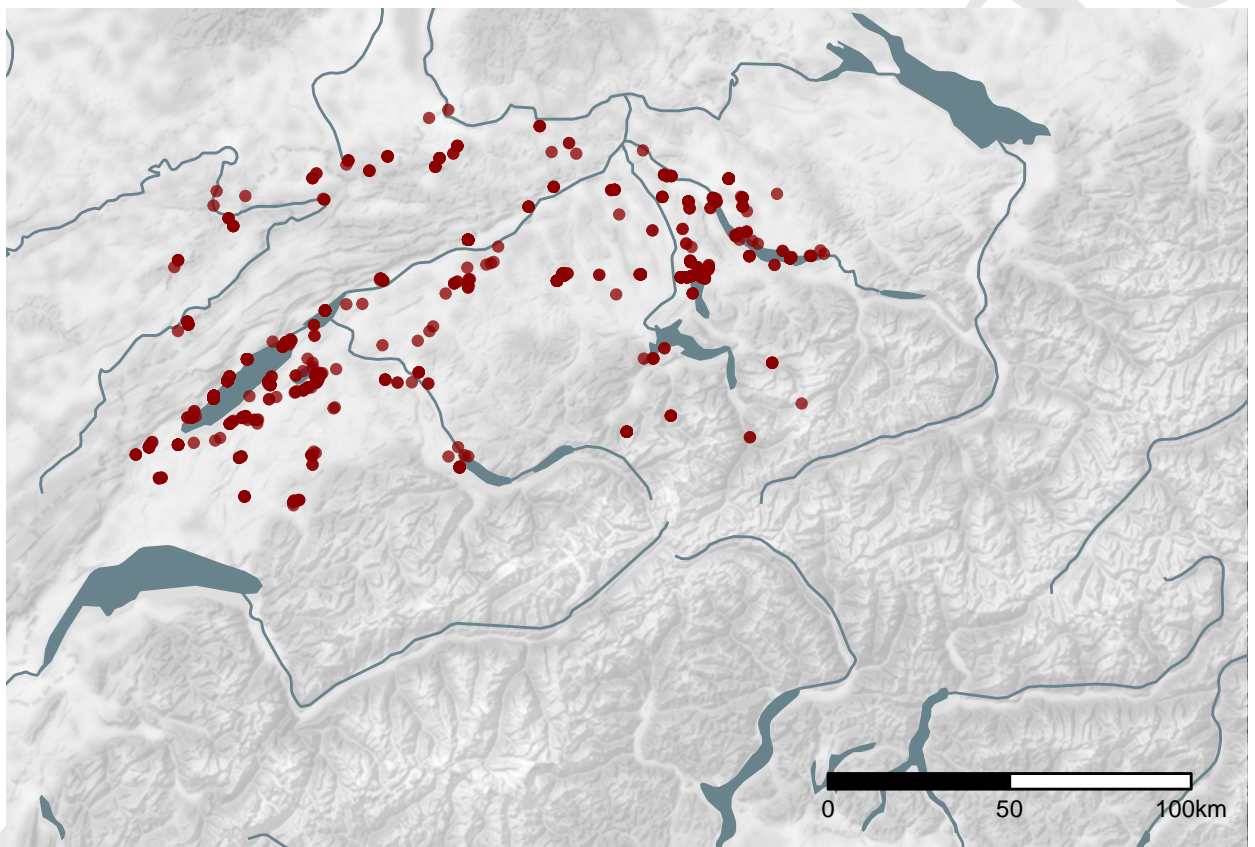


Figure 2: The location of the  $^{14}\text{C}$  dated sites in the dataset.

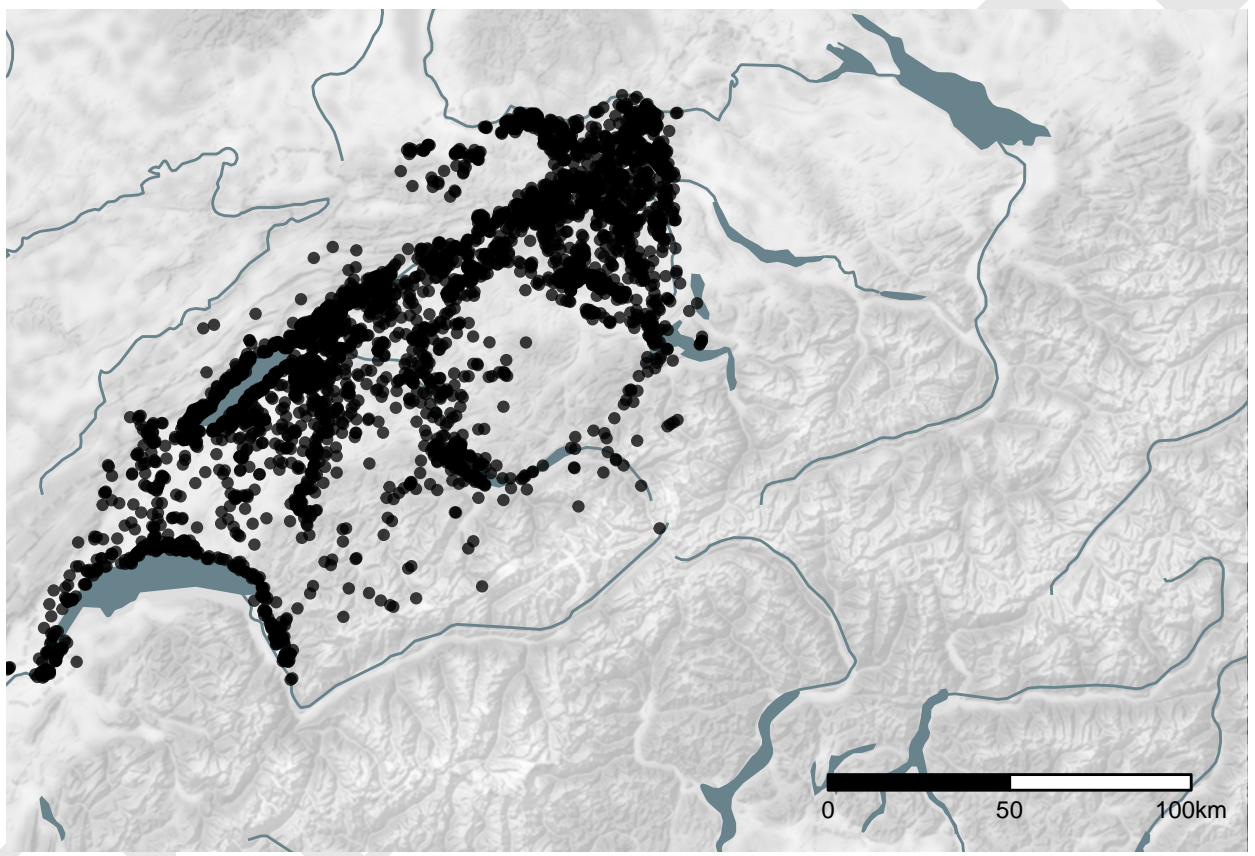


Figure 3: Location of the sites from the find reports of cantonal archaeology (heritage management) authorities. Locations are ‘fuzzed’ by approximately 1 km.

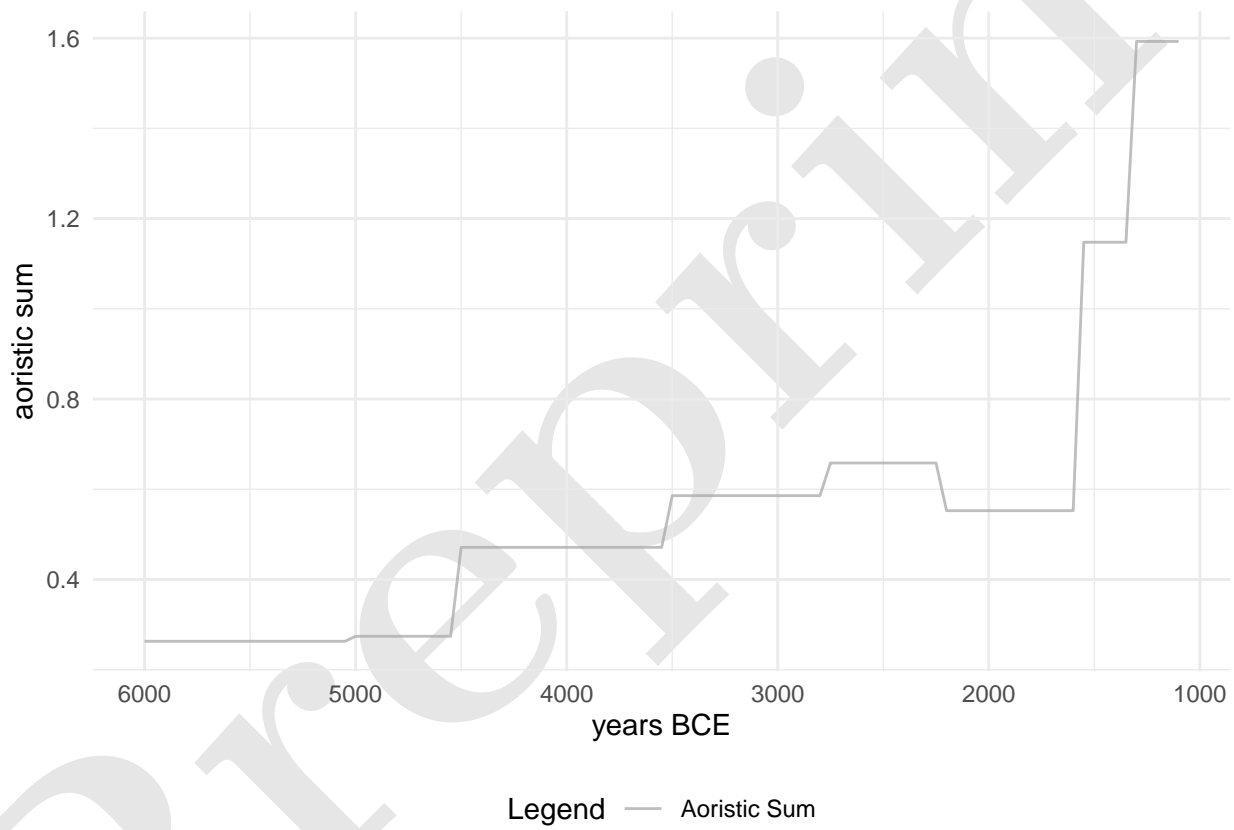


Figure 4: Aoristic sum of archaeological sites used in the analysis.

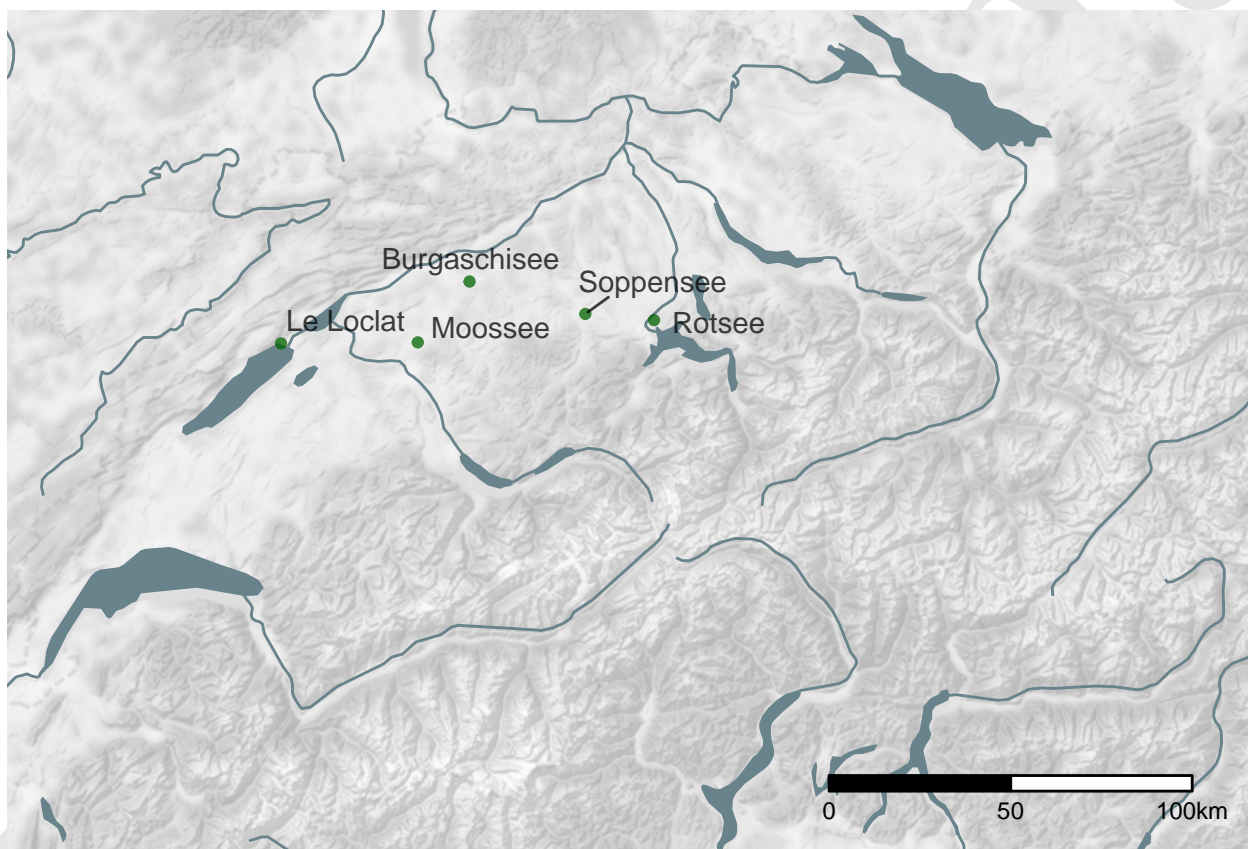


Figure 5: Location of the pollen profiles used for the openness indicator.

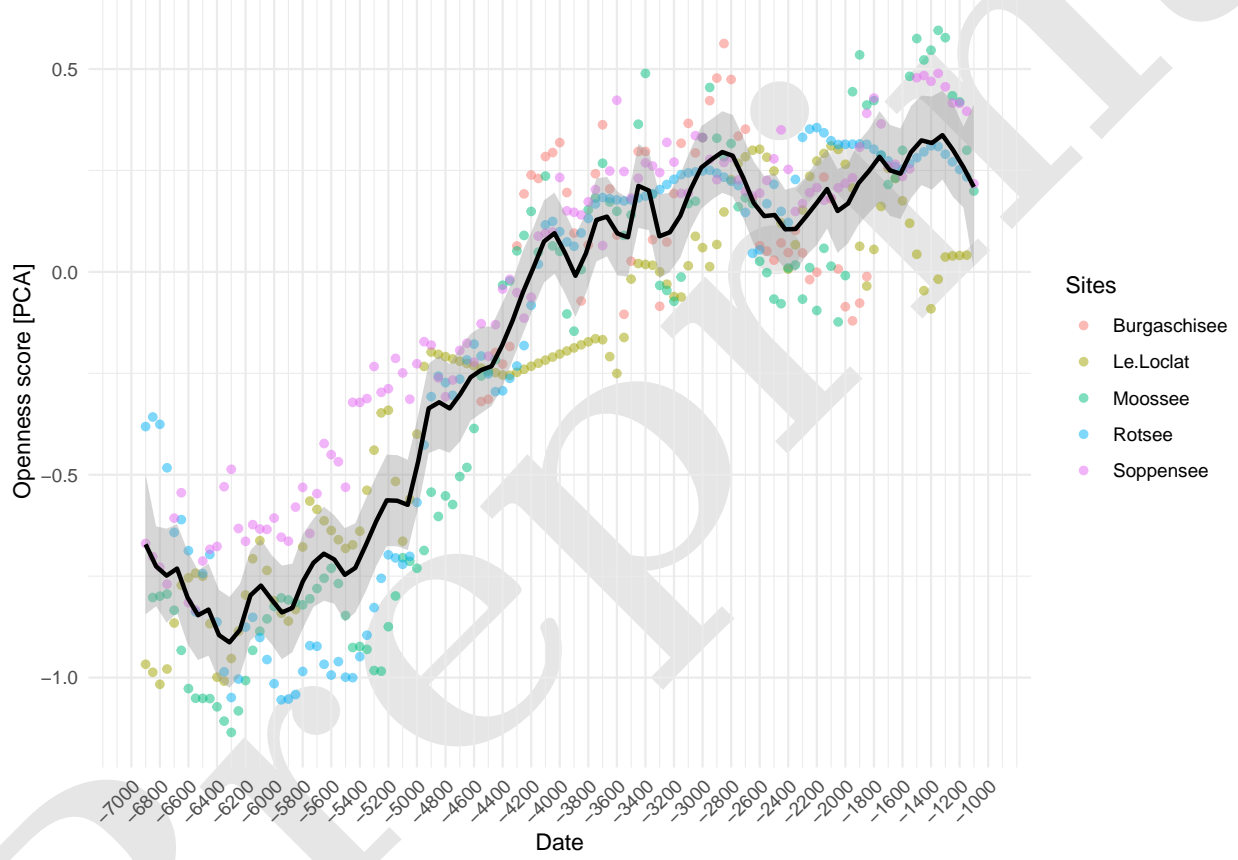


Figure 6: Value on the first dimension of the PCA against dating of the samples for the individual pollen profiles and their combined average value as the openness indicator.

205 **4. Methods: Bayesian model**

206 Sum calibration, openness and the dendro-dated settlement data was smoothed by a moving average with a  
207 50 years window, corresponding to the unified sampling interval for all proxies. The aoristic sum was not  
208 smoothed, because it already has a very coarse temporal resolution. In the construction of our ‘observational  
209 model’, we considered all these proxies as informative of the number of settlements located in the north of  
210 the Swiss Alps. Population development is simulated in a ‘process model’ using a Poisson process.

211 **4.1. Process model**

212 A special class of Bayesian hierarchical models are so-called ‘state space models’, specifically designed for  
213 time series. They follow two principles. First, a hidden or latent process is assumed, representing the state of  
214 the variable of interest  $x_t$  through the entire time series. Every state of variable  $x$  in the future, as well as in  
215 the past, is bound by a Markov process to the state of variable  $x$  at time  $t$ . Second, it is assumed that certain  
216 observations, represented in variable  $y$ , are dependent on the state of variable  $x$  at time  $t$ . This implies that  
217 a relationship between the individual states of variable  $y$  is generated over time via the hidden variable  $x$ ,  
218 which is not directly observable.

219 This structure makes these models particularly suitable for demographic reconstruction using archaeological  
220 and other data. Population density itself is not directly measurable: all we have at our disposal are observations  
221 derived by unknown transfer functions.

222 Our overall model is broken down into several hierarchically-connected individual elements. The a process  
223 model represents the demographic development itself, without already being explicitly parameterised with  
224 data. Here we assume that the latent variable ‘number of sites’ is strongly autocorrelated across different  
225 time periods. The number of sites in 3000 BCE is strongly conditioned by the number of sites in 3050 BCE,  
226 and so on. The population at time  $t$  results from the population at time  $t - 1$  times a parameter  $\lambda$ , which  
227 represents the population change at this time.

$$N_t = N_{t-1} * \lambda_t$$

228 A univariate discrete Poisson distribution is particularly suitable for modelling frequencies, numbers of events  
229 that occur independently of each other at a constant mean rate in a fixed time interval or spatial area. It is  
230 determined by a real parameter  $\lambda > 0$ , describing the expected value and the variance. Thus, the relationship  
231 shown above can be rearranged as follows:

$$\begin{aligned} N_t &\sim dpois(\lambda_t) \\ \lambda_t &= N_t \end{aligned}$$

232 If we now have information about the change in population development (the proxies), this can enter into the  
233 model via a change in  $\lambda$  in form of a regression: for all proxy values — represented as a vector of independent  
234 variables  $x \in R^n$ , with  $R^n$  as an n-dimensional Euclidean space defined by the n variables — the model takes  
235 the form:

$$\log(E(Y | x)) = \alpha + \beta'x$$

236 Using the logarithm as a link function ensures that  $\lambda$ , which must always be positive, can also be described  
237 by variables that may also be negative.  $\beta$  serves as slope factor, as in a normal linear regression. Here, it  
238 functions as a scaling factor for the individual proxies.  $\alpha$  is to be understood as an intercept, representing a  
239 baseline when there were no change due to the variables. This is the desired behaviour:  $\lambda$  is equal to the  
240 value of the population in the previous time period, plus or minus the changes resulting from the variables.

$$\log(\lambda_t) = \log(N_{t-1}) + \sum_{i=1}^n \beta_i x_{t,i}$$

241 Since  $\lambda$  and  $N$  are essentially in the same range (e.g. if  $lambda = 1$ , the expected value for  $N$  would also be 1),  
 242  $N_{t-1}$  must also be log-transformed for the congruence of both values. Population size  $N_t$  as well as population  
 243 change  $\lambda_t$  are time-dependent. At each individual point in time, these variables will take on different values.  
 244 But we can assume that the population change will not exceed certain limits (*max\_change\_rate*), though it  
 245 is not possible to specify this at this point.

$$\begin{aligned} max\_growth\_rate &\sim dgamma(shape = 5, scale = 0.05) \\ N_t/N_{t-1} &< (max\_growth\_rate + 1) \\ N_{t-1}/N_t &< (max\_growth\_rate + 1) \end{aligned}$$

246 A gamma distribution centres probability in the range  $[0, 1]$ ; adding 1 makes this range  $[1 - 2]$ . This prevents  
 247 the number of sites from explosively increasing between two time periods, which would lead to problems for  
 248 the convergence of the model. The estimation of this parameter for the entire model, as well as the estimation  
 249 of the respective population change per time section, results from the modelling and the interaction with the  
 250 data.

## 251 4.2. Observational model

252 In this initial implementation, the observational model is essentially a Poisson regression, where the proxies  
 253 are used to inform the change in the number of settlements between time steps. The individual proxies were  
 254 z-normalised and absolute differences between time steps were then computed. If the value of the proxy  
 255 increases, this results in a positive difference from the previous time step, and vice versa.

$$\begin{aligned} z_t &= \frac{x_t - \bar{x}}{\sigma_x} \mid \sigma_x := Standard\ Deviation \\ \delta z_t &= z_t - z_{t-1} \end{aligned}$$

256 The sum of the resulting differences between the time steps, together with the settlement number of the  
 257 previous step as the expected value, then forms  $\lambda_t$ : the expected value for the settlement number of the  
 258 current time step.

$$\log(\lambda_t) = \log(N_{t-1}) + \sum_{i=1}^n \beta_i \delta z_{i,t}$$

259 Here,  $\beta_i$  is a scaling factor that represents the influence of the respective proxy. It is a confidence value of the  
 260 model for the respective proxy, so that the sum of all  $\beta_i$  results in 1.

$$\sum_{i=1}^n \beta_i = 1$$

261 A Dirichlet distribution—a multivariate generalization of the beta distribution—is commonly used for  
 262 this purpose in hierarchical Bayesian modelling. Its density function gives the probabilities of  $i$  different  
 263 exclusive events. It has a parameter vector  $\alpha = (\alpha_1, \dots, \alpha_i) \mid (\alpha_1, \dots, \alpha_i) > 0$ , for which we have chosen a  
 264 weakly informative log-normal prior. The priors for the log-normal distribution in turn come from a weakly  
 265 informative exponential distribution for the mean and a log-nomal distribution with  $\mu$  of 1 and  $\sigma_{log}$  of 0.1:

$$\begin{aligned}
\beta_i &\sim Dir(\alpha_{1-i}) \\
\alpha_i &\sim LogNormal(\mu_{alpha_i}, \sigma_{alpha_i}) \\
\mu_{alpha_i} &\sim Exp(1) \\
\sigma_{alpha_i} &\sim LogNormal(1, 0.1)
\end{aligned}$$

266 Intuitively, we consider the sum of the proxies as determinant of the number of settlements. That is, the  
267 share of each individual proxy is variable and is estimated within the model. This share is recorded within  
268 the model as the parameter p.

269 The error value is represented by the Poisson process in the process model. In this implementation, the model  
270 finds the best possible combination between the individual proxies to describe a settlement dynamic. The  
271 number of sites is converted into population density using (certainly debatable) parameters defined by us,  
272 but which are only scaling factors for the intermediate value of number of settlements. We assume that each  
273 site represents a number of people that is poisson distributed around the value 50, a compromise, as both  
274 Mesolithic and Neolithic and Bronze Age settlement communities need to be represented. An evidence-based  
275 estimate data series of the temporal development of settlement sizes could enhance this specification. From  
276 the number of sites and the mean number of individuals a population density can be calculated using the  
277 case study area ( $12649 \text{ km}^2$ ), making the models estimate comparable with estimates from other sources or  
278 the literature.

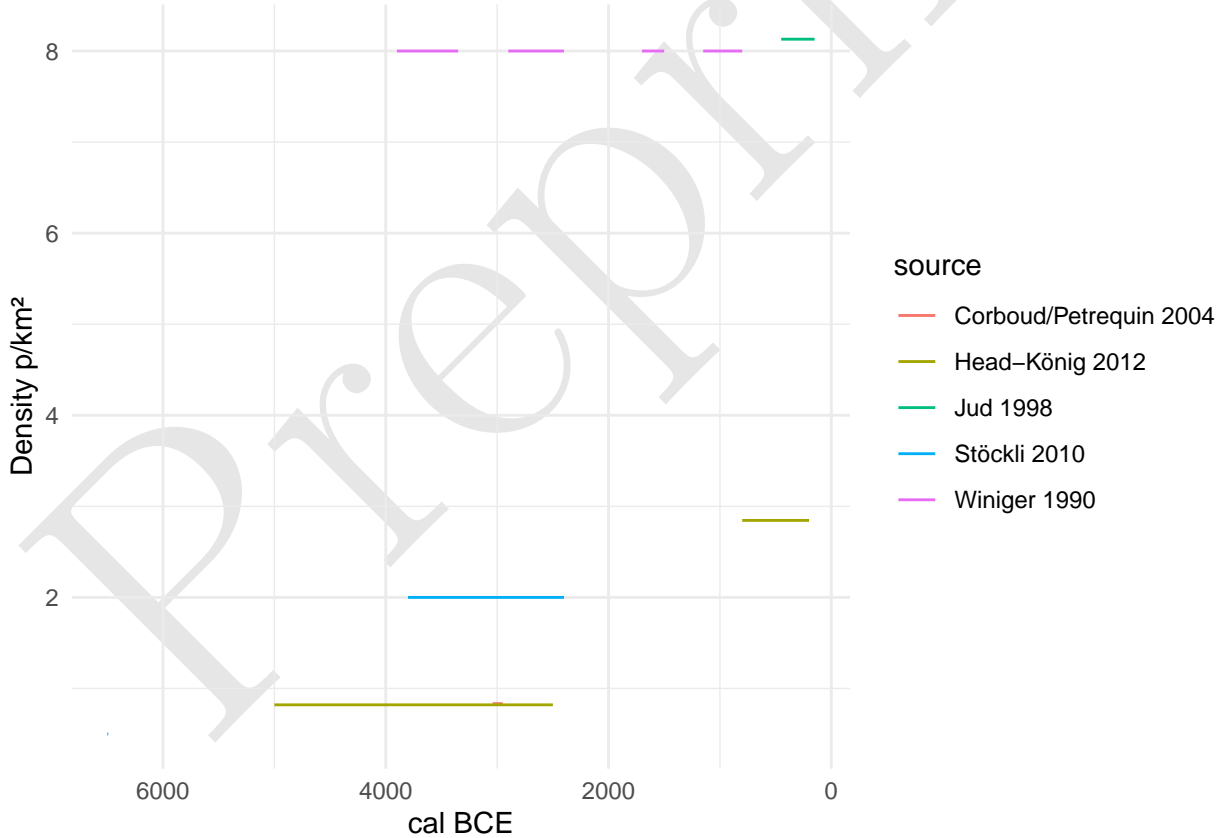


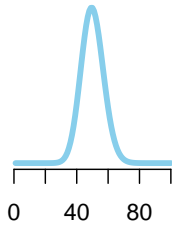
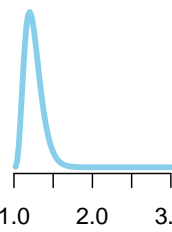
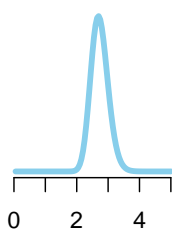
Figure 7: Expert estimate of population density on the Swiss Plateau.

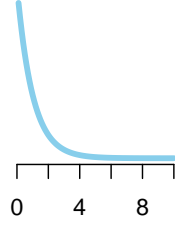
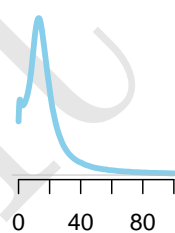
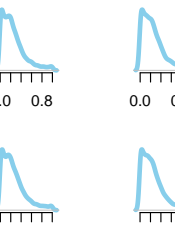
### 279 4.3. Model fitting

280 The model was fitted using the R package *nimble* (version 0.11.1, R version 4.1.3), using 4 parallel chains.  
281 Achieving and ensuring convergence and sufficient effective samples (10000) for a reliable assessment of the

282 highest posterior density interval was carried out in steps.  
 283 1) the model was initialised for each chain and run for 100000 iterations (with a thinning of 10). On a  
 284 reasonably capable computer (Linux, Intel(R) Xeon(R) CPU E3-1240 v5 @ 3.50GHz, 4 cores, 8 threads),  
 285 this takes approximately a minute.  
 286 2) the run was extended until convergence could be determined using Gelman and Rubin's convergence  
 287 diagnostic, the criterion being that a potential scale reduction factor of less than 1.1 was achieved for  
 288 all monitored variables. Convergence occurred after about thirty seconds.  
 289 3) Due to the high correlation of the parameters and thus a low sampling efficiency, the collection of at  
 290 least 10,000 effective samples for all parameters took about five hours.  
 291 A starting value of 5 p/km<sup>2</sup> for the population density of the Late Bronze Age (1000 BCE) was taken from  
 292 the literature, which may represent a general average value for all prehistoric population estimates (Nikulka,  
 293 2016, p. 258). For the model, this was set as the mean of a normal distribution with a standard deviation of  
 294 0.5, which should give enough leeway for deviations resulting from the data. Nevertheless, it should be noted  
 295 that our resulting estimate is strongly conditioned by this predefined value, especially in the later sections.  
 296 For traceplots and the prior-posterior overlap, as well as density functions of the posterior samples of the  
 297 individual parameters, please refer to the supplementary material.

Table 2: Priors and fixed parameters used in the model.

Priors	Value	Plot/Comment
MeanSiteSize	dpois(50)	
max_growth_rate	dgamma(shape = 5, scale=0.05) + 1	
mu_alpha	dlnorm(1,sdlog=0.1)	

Priors	Value	Plot/Comment
a_alpha	dexp(1)	
alpha	dlnorm(mu_alpha[j],sdlog=a_alpha[j])	
p	ddirch(alpha[1:4])	
<b>Parameters</b>		
nEnd	5	
AreaSwissPlateau	12649 km <sup>2</sup>	
<b>Initial Values</b>		
lambda <sub>1:nYears</sub>	$\log(1 - 10^{\frac{1}{nYears-1}})$	exponential increase of the factor 10
PopDens <sub>1:nYears</sub>	nEnd (=5)	
nSites <sub>1:nYears</sub>	50	

## 298 5. Results

299 The population density estimated by the model (Figure 8) ranges between 0.2 p/km<sup>2</sup> for the beginning (6000  
300 BCE) and 4.8 p/km<sup>2</sup> for the end of the estimate (1000 BCE), reaching a maximum of 6.5 p/km<sup>2</sup> for around  
301 1250 BCE. This remains within the range considered plausible according to expert estimates. There are  
302 clear peaks around 1250 BCE and around 2750 BCE, which corresponds to the beginning of the influence of  
303 Corded Ware ceramic styles (Hafner, 2004).

304 The temporal distribution of variability in the estimate (Figure 9) allows us assess at which time steps the  
305 uncertainty is greater due to e.g. contradictions in the proxies. The coefficient of variation is 0.13 for the  
306 beginning and 0.1 for the end of the estimate, with the greatest variability (0.47) seen around 2150 BCE.  
307 This is not surprising as there are fewer archaeological contexts recorded from the earlier phase of the Early  
308 Bronze Age, c. 2200-1800 BCE. This picture changes from c. 1800 BCE onwards (David-Elbiali, 2000; Hafner,  
309 1995). The beginning and end of the time series are relatively clearly determined, resulting from the *a priori*  
310 setting of final population density, but also from the uniformity of the proxies during these periods. Overall,

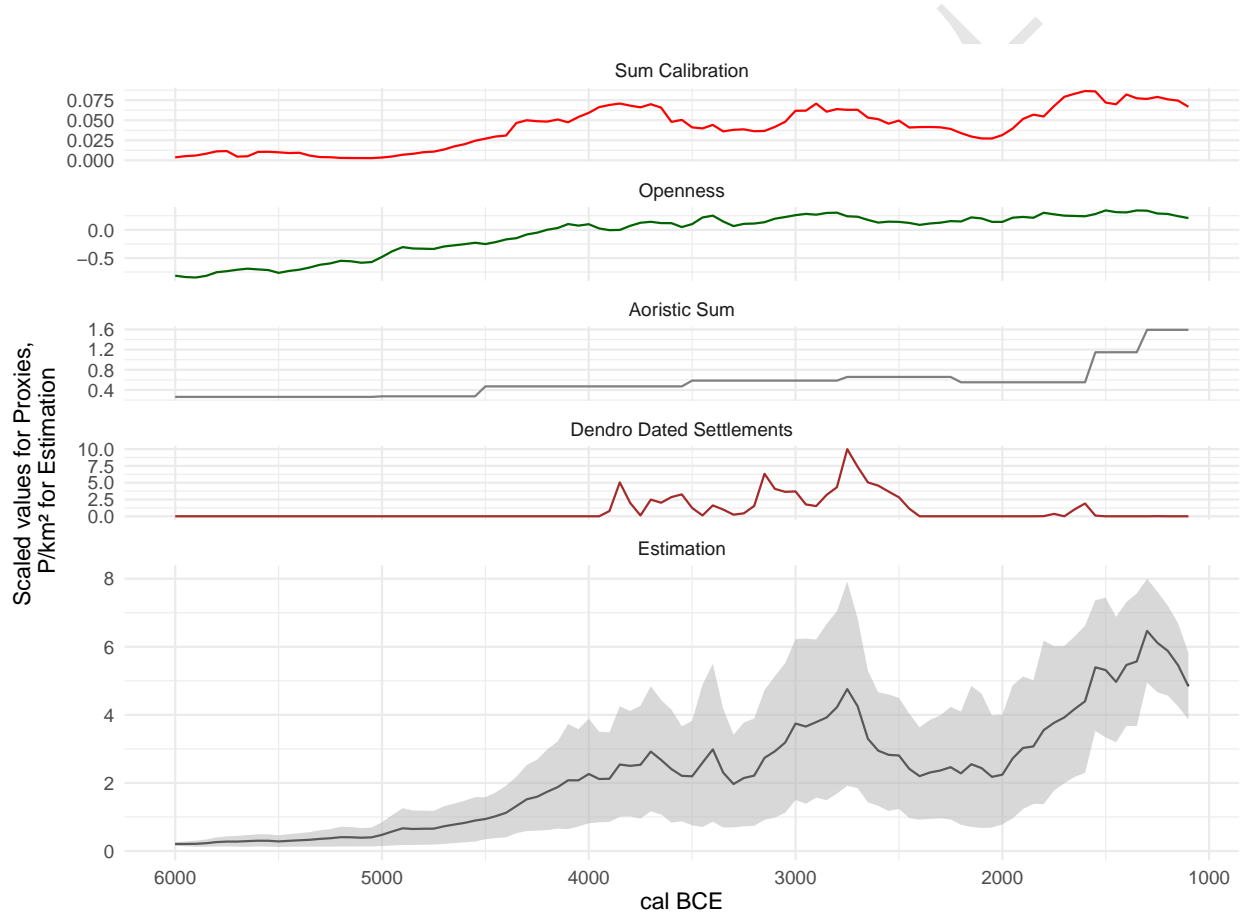


Figure 8: Estimate of population density predicted by the model. The four input proxies are also plotted (scaled) for comparison.

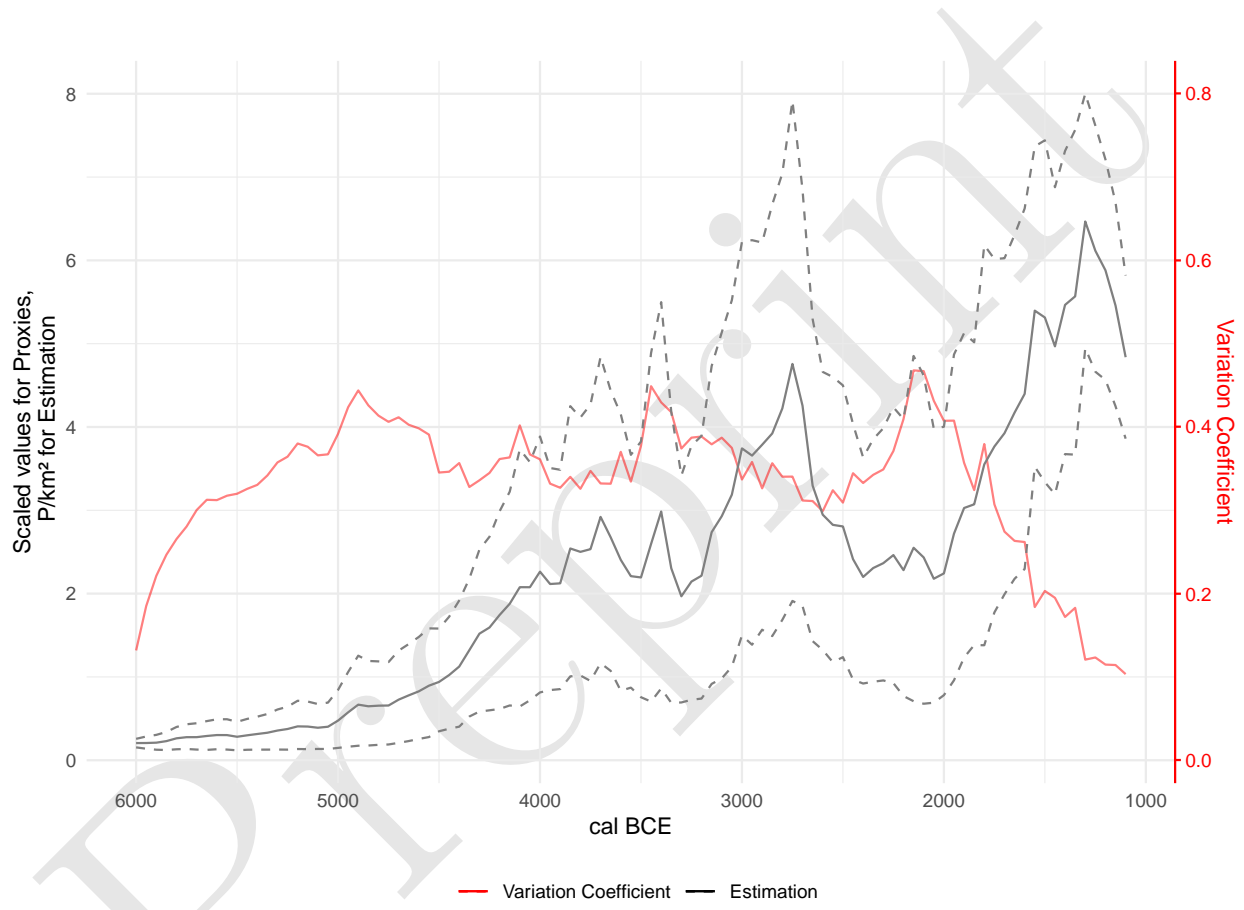


Figure 9: Variability of the model estimate of population density over time, with the estimate itself for reference.

311 the variability is relatively stable over the entire estimation and averages 33% of the respective mean.

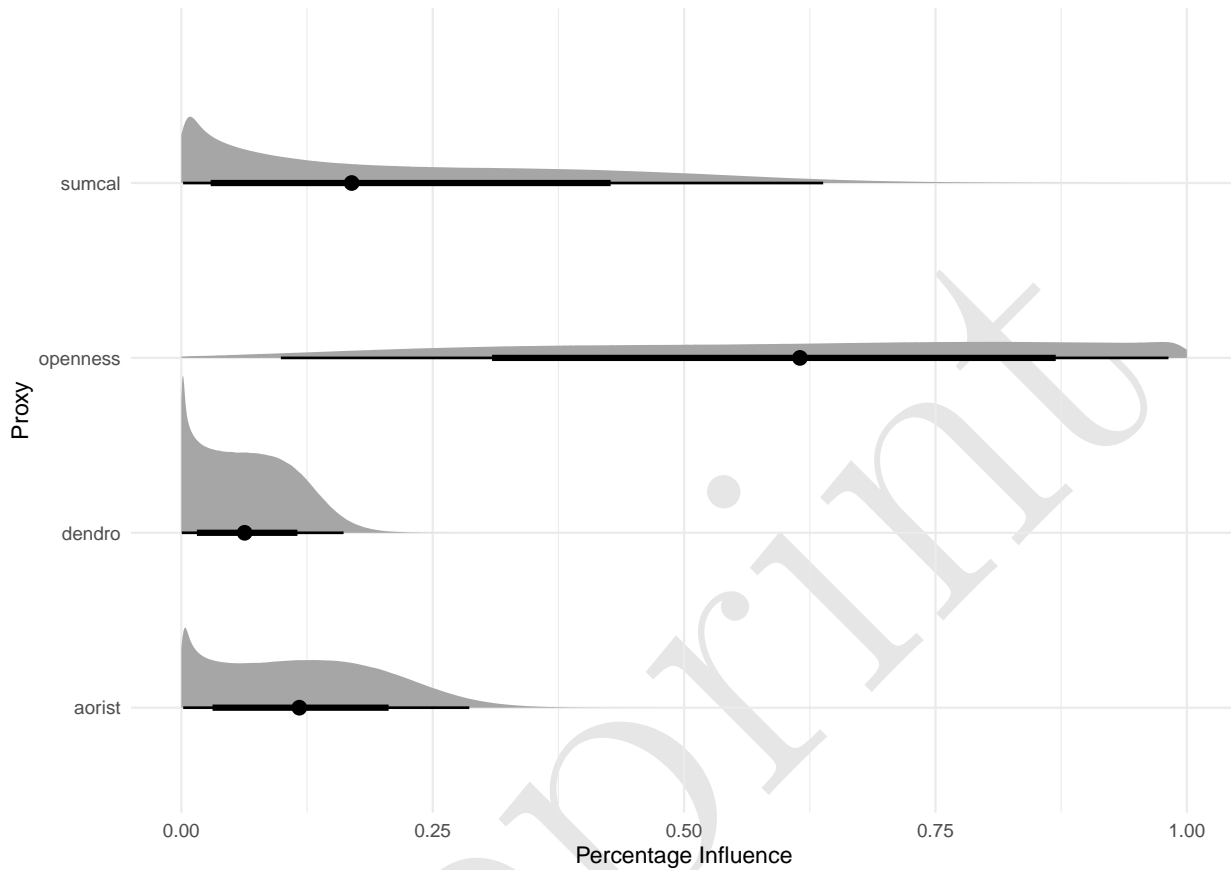


Figure 10: Distribution of influence ratios of proxies on model's final estimation of number of sites.

312 The parameter  $p$  reflects the relative weight given to the individual proxies. Its posterior distribution (Figure  
313 10) shows that the model weights the openness indicator the highest, averaging slightly above 60%, followed  
314 by the sum calibration, with an average of about 20%. The aoristic sum is slightly above 10%, whereas the  
315 importance of the dendro-dated settlements is below 10%. The reason for the latter is certainly that there  
316 are no lakeshore settlements over large areas of the time window, and therefore the overall confidence in the  
317 proxy is low. The aoristic sum is flat for long periods, making it difficult to integrate with other proxies. The  
318 sum calibration shows very strong short-term fluctuations, at least partly due to the calibration curve, which  
319 suggests that it does not reliably represent a continuous population trend. Its fluctuations have an impact on  
320 the model's estimate, albeit to a lesser extent than the general trend.

## 321 6. Discussion

### 322 6.1. Reliability of individual proxies

323 Comparing the model's overall estimate with the individual proxies provides several insights into the quality  
324 of these records. The sum calibration, currently the most frequently used proxy for (relative) population  
325 change in prehistory, has its large fluctuations dampened when considered alongside other proxies. This  
326 is especially true of the first fluctuation shortly after 4000 BCE. The expected increase in archaeological  
327 remains with the onset of Neolithisation is still clearly visible, but the overall curve is much flatter than  
328 the sum calibration itself. The period between 3950 and 3700 BCE, contemporaneous with the first major  
329 settlement of the Three Lakes regions' lakeshores, coincides with a noticeable plateau in the calibration curve,

330 producing an overestimation of the  $^{14}\text{C}$  density. A second maximum, after 3000 BCE, is supported by the  
331 other proxies, and is consequently much more reflected in the overall estimate, coinciding with a smaller and  
332 shorter plateau. The rise towards the Middle and Late Bronze Age is also supported by the other proxies,  
333 without a significant pattern in the calibration curve. We may conclude that the model is successful in using  
334 information from other proxies to sift ‘real’ fluctuations in the summed radiocarbon record from artefacts of  
335 the calibration curve.

336 On average, the model weights the sum calibration at about 20%, significantly less than the 60% afforded  
337 to the openness indicator. After an initial increase, which is easily explained by spread of agriculture, the  
338 openness indicator tends to fluctuate less and thus has a dampening effect on the overall estimate. In general,  
339 this trend in the sum calibration is well reflected in land openness, while changes within the Neolithic and  
340 Bronze Age are more gradual.

341 The aoristic sum remains flat over long spans of time. It is not until the Middle and Late Bronze Age that  
342 we see a significant rise, which is also apparent in the model’s overall estimate. It remains to be seen to what  
343 extent modelling of the taphonomic loss (Surovell et al., 2009) could be integrated in this approach.

344 The number of simultaneously existing lakeshore settlements is a temporally and spatially limited estimator,  
345 but extremely reliable. Its limitations are reflected in the low overall confidence of the model, since its value  
346 is zero over long stretches. However, where it has information potential, such as around and shortly after  
347 3800 BCE, 3200 BCE, 1600 BCE or especially around 2750 BCE, its fluctuations have a noticeable influence  
348 on the overall estimate. This highlights another potential of our approach: where a proxy has little structure  
349 and thus little significance, or where its trends cannot be linked to other indicators, it consequently has little  
350 influence. For periods in which it can provide information, however, this will also feed into the overall model,  
351 despite a low overall confidence in the estimator.

## 352 **6.2. Prehistoric population dynamics north of the Swiss Alps**

353 In order to review the reconstruction against the background of established archaeological knowledge, it is  
354 useful to overlay conventionally-defined archaeological phase boundaries (Hafner, 2005) on the results of our  
355 model (Figure 11).

356 The Early and Middle Neolithic are hardly documented in Switzerland. We must assume a low level of  
357 settlement, probably mainly by mobile groups. Isolated Neolithic sites of the LBK and later groups are known  
358 in the periphery of Switzerland, but they play a subordinate role (Ebersbach et al., 2012). The evidence  
359 of the Neolithic is dense from the so-called Upper Neolithic onwards, connected with the typochronological  
360 pottery phases of Egolzwil (late 5th millennium BCE) and Cortaillod respectively Pfyn (first half of the  
361 4th millennium BCE). The first lake shore settlements north of the Alps date to this time too. Here we  
362 see a clear increase in the estimated population in the model. In the transition to the Late Neolithic, we  
363 know from the lakeshore settlements the so-called Horgen Gap (Hafner, 2005). This is also visible as a slight  
364 decrease in the model. In another study (Heitz et al., 2021) we demonstrated that this is in fact probably not  
365 a decline in population. Rather communities relocated their settlements to the hinterland of the large lakes  
366 in times of stronger lake level rises due to climatic changes. In the Late Neolithic, associated with the Horgen  
367 pottery, we then see a clear increase in the settlement intensity, which peaks and breaks off at the transition  
368 to the Final Neolithic (Hafner, 2004). In the second half of the Early Bronze Age, during which lakeshores  
369 were resettled to a smaller extend, there is again a clear increase in population size according to the model,  
370 continuing until the Late Bronze Age. The general trends fit very well with the previous reconstructions of  
371 population development for Switzerland (see eg. Lechterbeck et al., 2014), while offering higher precision and  
372 higher resolution.

## 373 **7. Conclusions**

374 The key advance in the model we present is the ability to estimate, in absolute terms, past population  
375 sizes and the uncertainty accompanying our present knowledge. These estimates can be a basis for further  
376 studies where relative measures of population development are not helpful, such as long-term land use studies.

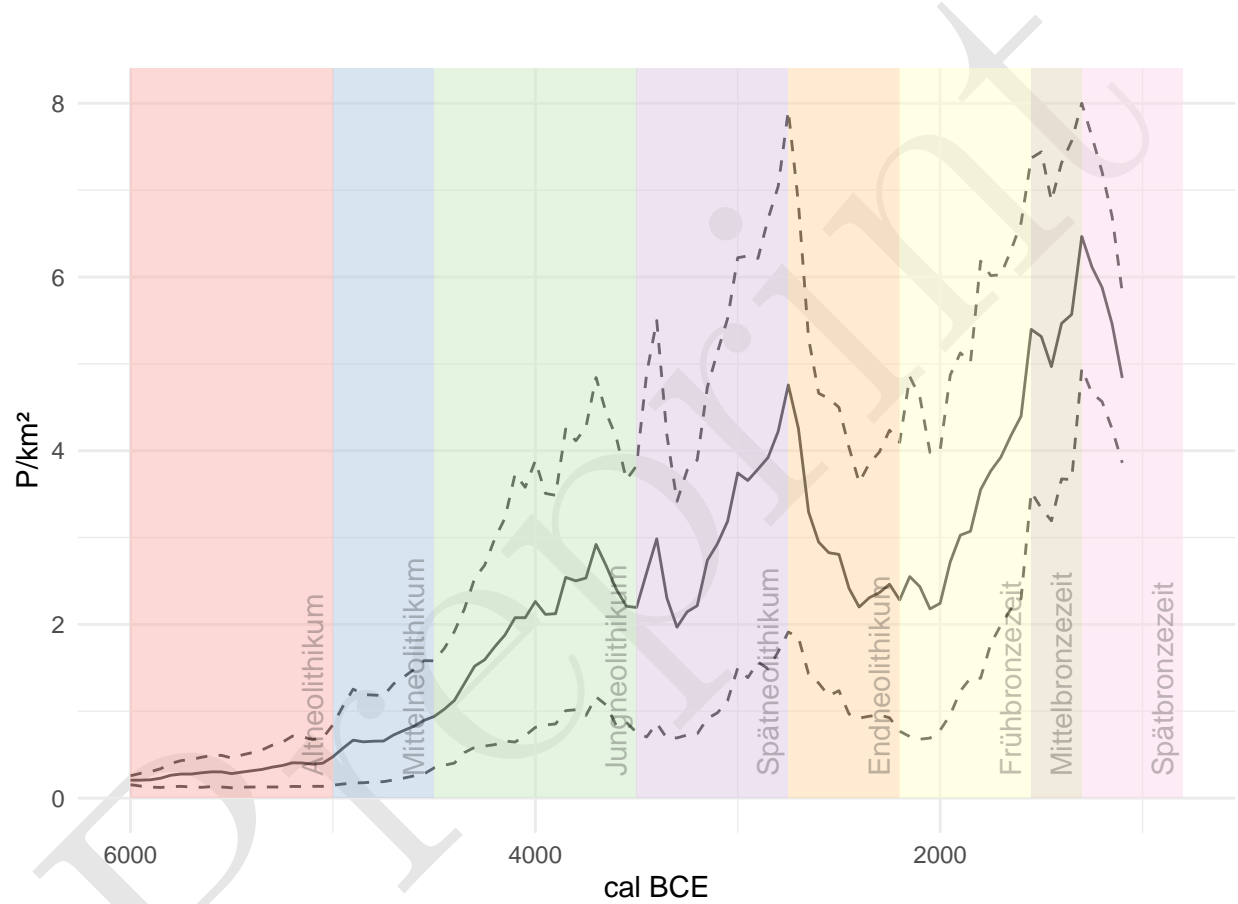


Figure 11: Estimate of population density in relation to the established chronology of the case study area north of the Swiss Alps.

377 Modelling of large-scale socio-ecological systems based on archaeological data does not have to rely deductive,  
378 asynchronous population models (e.g. carrying capacity or ethnographic analogues).

379 We have also demonstrated that, with Bayesian hierarchical modelling, it is possible to achieve a true  
380 multi-proxy analysis – as opposed to a juxtaposition of different indicators. This opens up the possibility  
381 of quantitatively linking different records and assessing their credibility. We are also able to specifying a  
382 confidence interval for the overall estimate. The result is a firmer basis for reconstructing population dynamics  
383 and settlement patterns in prehistory.

384 Nevertheless, we consider this model as only the first step towards a more sophisticated Bayesian approach.  
385 We have trusted the individual proxies in aggregate, without individualised measurement error. Our estimates  
386 are based on a limited number of sources, almost all of which are subject to taphonomic biases in the  
387 archaeological record. Consequently, we can only transform the model’s prediction into an absolute estimate  
388 of population density with predefined parameters: settlement size and the initial value of the reconstruction.  
389 Overcoming this limitation would represent a major refinement of our approach.

390 Incorporating additional proxies independent of the immediate, time-dependent conditions of the archaeological  
391 record could be one way to achieve this. These could be data on settlement sizes, parameters for economic-  
392 ecological carrying capacity, demographic data from burial groups or archaeogenetic data on population sizes.  
393 This data is available to varying degrees in different regions. On the Swiss Plateau, for example, we have little  
394 data on human remains over large spans of prehistory, in contrast to the abundance of wetland settlements.

395 To apply this approach to other regions, the proxies we use here would have to be adapted to fit local  
396 conditions and research histories. By means of large-scale modelling, however, it would be possible to  
397 supplement gaps in the data in one region with data from another by regionalisation and a partial transfer of  
398 information (partial pooling). Such an extension would be the next logical step in the improvement of the  
399 model, to which end we hope to be able to contribute a further study in the near future.

## 400 8. Acknowledgements

401 Data collection were conducted as part of the project ‘Beyond lake settlements’ in the doctoral thesis of Julian  
402 Laabs, funded by the SNF (project number 152862, PI Albert Hafner) and as part of the XRONOS project,  
403 also funded by the SNSF (project number 198153, PI Martin Hinz). The development of the openness index  
404 took place within the framework of the project Time and Temporality in Archaeology (project number 194326,  
405 PI Caroline Heitz), inspired by the cooperation within the project QuantHum (project 169371, PI Marco  
406 Conedera), both also funded by the SNSF. Jan Kolář was supported by a long-term research development  
407 project (RV67985939) and by a grant from the Czech Science Foundation (19-20970Y). We also thank the  
408 Institute of Archaeological Sciences of the University of Bern for its support and faith in the outcome of our  
409 modelling project. Finally, we thank (already) the unknown reviewers for their helpful comments, which will  
410 certainly improve this manuscript significantly.

## 411 9. Code availability

412 The computer code used to generate the Bayesian Population model is provided in full in the Supplementary  
413 Information, together with information about the program and version used. The R code and Data are  
414 available online at <https://github.com/MartinHinz/bayesian.demographic.reconstruction.2022> and is archived  
415 at <https://doi.org/10.5281/zenodo.6594498>.

## 416 10. References

- 417 Attenbrow, V., Hiscock, P., 2015. Dates and demography: Are radiometric dates a robust proxy for long-term  
418 prehistoric demographic change? *Archaeology in Oceania* 50, 30–36. <https://doi.org/10.1002/arco.5052>
- 419 Bryant, J., Zhang, J.L., 2018. Bayesian Demographic Estimation and Forecasting. Chapman; Hall/CRC.  
420 <https://doi.org/10.1201/9780429452987>
- 421 Carleton, W.C., Groucutt, H.S., 2021. Sum things are not what they seem: Problems with point-wise  
422 interpretations and quantitative analyses of proxies based on aggregated radiocarbon dates. *The Holocene*  
423 31, 630–643. <https://doi.org/10.1177/0959683620981700>
- 424 Childe, V.G. (Ed.), 1936. *Man Makes Himself*. Watts & Co., London.
- 425 Christian Lüthi, 2009. Mittelland (region).
- 426 Crema, E.R., 2022. Statistical Inference of Prehistoric Demography from Frequency Distributions of  
427 Radiocarbon Dates: A Review and a Guide for the Perplexed. *Journal of Archaeological Method and*  
428 *Theory*. <https://doi.org/10.1007/s10816-022-09559-5>
- 429 Crema, E.R., Bevan, A., 2021. Inference from large sets of radiocarbon dates: software and methods.  
430 *Radiocarbon* 63, 23–39. <https://doi.org/10.1017/RDC.2020.95>
- 431 Crema, E.R., Shoda, S., 2021. A Bayesian approach for fitting and comparing demographic growth models  
432 of radiocarbon dates: A case study on the Jomon-Yayoi transition in Kyushu (Japan). *PloS One* 16,  
433 e0251695. <https://doi.org/10.1371/journal.pone.0251695>
- 434 David-Elbiali, M., 2000. La Suisse occidentale au IIe millénaire av. J.-C. : Chronologie, culture, intégration  
435 européenne. *Cahiers d'archéologie romande*, Lausanne.
- 436 Ebersbach, R., Kühn, M., Stopp, B., Schibler, J., 2012. Die Nutzung neuer Lebensräume in der Schweiz  
437 und angrenzenden Gebieten im 5. Jtsd. V. Chr. : Siedlungs- und wirtschaftsarchäologische Aspekte.  
438 *Jahrbuch Archäologie Schweiz* 95, 7–34. <https://doi.org/10.5169/SEALS-392483>
- 439 French, J.C., Riris, P., Fernandéz-López de Pablo, J., Lozano, S., Silva, F., 2021. A manifesto for palaeodemography  
440 in the twenty-first century. *Philosophical Transactions of the Royal Society B: Biological*  
441 *Sciences* 376, 20190707. <https://doi.org/10.1098/rstb.2019.0707>
- 442 Hafner, A., 2005. Neolithikum: Raum/Zeit-Ordnung und neue Denkmodelle. *Archäologie im Kanton Bern*  
443 6B, 431–498.
- 444 Hafner, A., 2004. Vom Spät- zum Endneolithikum. Wandel und Kontinuität um 2700 v. Chr. In *Mitteleuropa.*  
445 - Vom Endneolithikum zur Frühbronzezeit: Wandel und Kontinuität zwischen 2400 und 1500 v.Chr, in:  
446 Beier, H.J., Einicke, R. (Eds.), *Varia Neolithica. 3. Beiträge Zur Ur- Und Frühgeschichte Mitteleuropas.*  
447 Beier&Beran, Weissbach, pp. 213–249.
- 448 Hafner, A., 1995. Die Frühe Bronzezeit in der Westschweiz. Funde und Befunde aus Siedlungen, Gräbern  
449 und Horten der entwickelten Frühbronzezeit. *Staatlicher Lehrmittelverlag Bern* 1995, Bern.
- 450 Hassan, F.A., 1981. Demographic archaeology, Studies in archaeology. Academic Press, New York.
- 451 Heitz, C., Hinz, M., Laabs, J., Hafner, A., 2021. Mobility as resilience capacity in northern Alpine Neolithic  
452 settlement communities. <https://doi.org/10.17863/CAM.79042>
- 453 Kintigh, K.W., Altschul, J.H., Beaudry, M.C., Drennan, R.D., Kinzig, A.P., Kohler, T.A., Limp, W.F.,  
454 Maschner, H.D.G., Michener, W.K., Pauketat, T.R., Peregrine, P., Sabloff, J.A., Wilkinson, T.J., Wright,  
455 H.T., Zeder, M.A., 2014. Grand challenges for archaeology. *Proceedings of the National Academy of*  
456 *Sciences* 111, 879–880. <https://doi.org/10.1073/pnas.1324000111>
- 457 Kruschke, J.K., 2015. Doing Bayesian Data Analysis. Elsevier. <https://doi.org/10.1016/B978-0-12-405888-0.09999-2>
- 458 Laabs, J., 2019. Populations- und landnutzungsmodellierung der neolithischen und bronzezeitlichen  
459 westschweiz (PhD thesis). Bern.
- 460 Lechterbeck, J., Edinborough, K., Kerig, T., Fyfe, R., Roberts, N., Shennan, S., 2014. Is Neolithic land  
461 use correlated with demography? An evaluation of pollen-derived land cover and radiocarbon-inferred  
462 demographic change from Central Europe. *The Holocene* 24, 1297–1307. <https://doi.org/10.1177/0959683614540952>
- 463 Martínez-Grau, H., Morell-Rovira, B., Antolín, F., 2021. Radiocarbon Dates Associated to Neolithic Contexts  
464 (Ca. 5900 – 2000 Cal BC) from the Northwestern Mediterranean Arch to the High Rhine Area. *Journal*  
465 *of Open Archaeology Data* 9, 1. <https://doi.org/10.5334/joad.72>
- 466 Morris, I., 2013. The measure of civilization: How social development decides the fate of nations. Princeton

- 469 University Press, Princeton.
- 470 Müller, J., Diachenko, A., 2019. Tracing long-term demographic changes: The issue of spatial scales. PLOS  
471 ONE 14, e0208739. <https://doi.org/10.1371/journal.pone.0208739>
- 472 Nikulka, F., 2016. Archäologische Demographie. Methoden, Daten und Bevölkerung der europäischen Bronze-  
473 und Eisenzeiten. Sidestone Press, Leiden.
- 474 Ramsey, C.B., 1995. Radiocarbon calibration and analysis of stratigraphy; the OxCal program. Radiocarbon  
475 37, 425430.
- 476 Rick, J.W., 1987. Dates as Data: An Examination of the Peruvian Preceramic Radiocarbon Record. American  
477 Antiquity 52, 55–73. <https://doi.org/10.2307/281060>
- 478 Riede, F., 2009. Climate and demography in early prehistory: Using calibrated (14)C dates as population  
479 proxies. Human Biology 81, 309–337. <https://doi.org/10.3378/027.081.0311>
- 480 Schmidt, I., Hilpert, J., Kretschmer, I., Peters, R., Broich, M., Schiesberg, S., Vogels, O., Wendt, K.P.,  
481 Zimmermann, A., Maier, A., 2021. Approaching prehistoric demography: Proxies, scales and scope of the  
482 Cologne Protocol in European contexts. Philosophical Transactions of the Royal Society B: Biological  
483 Sciences 376, 20190714. <https://doi.org/10.1098/rstb.2019.0714>
- 484 Shennan, S., 2000. Population, Culture History, and the Dynamics of Culture Change. Current Anthropology  
485 41, 811–835.
- 486 Shennan, S., Downey, S.S., Timpson, A., Edinborough, K., Colledge, S., Kerig, T., Manning, K., Thomas,  
487 M.G., 2013. Regional population collapse followed initial agriculture booms in mid-Holocene Europe.  
488 Nature Communications 4, 2486. <https://doi.org/10.1038/ncomms3486>
- 489 Surovell, T.A., Byrd Finley, J., Smith, G.M., Brantingham, P.J., Kelly, R., 2009. Correcting temporal  
490 frequency distributions for taphonomic bias. Journal of Archaeological Science 36, 1715–1724. <https://doi.org/10.1016/j.jas.2009.03.029>
- 492 Turchin, P., Brennan, R., Currie, T., Feeney, K., Francois, P., Hoyer, D., Manning, J., Marciniak, A., Mullins,  
493 D., Palmisano, A., Peregrine, P., Turner, E.A.L., Whitehouse, H., 2015. Sesat: The Global History  
494 Databank. Cliodynamics 6. <https://doi.org/10.21237/C7clio6127917>
- 495 Zimmermann, A., 2004. Landschaftsarchäologie II. Überlegungen zu prinzipien einer landschaftsarchäologie.

## 496 11. Author contributions

- 497 • *Martin Hinz*: Conceptualization, Methodology, Software, Validation, Formal analysis, Investigation,  
498 Data Curation, Writing - Original Draft, Writing - Review & Editing, Visualization  
499 • *Joe Roe*: Software, Validation, Writing - Review & Editing  
500 • *Julian Laabs*: Investigation, Data Curation, Writing - Review & Editing  
501 • *Caroline Heitz*: Conceptualization, Investigation, Writing - Review & Editing  
502 • *Jan Kolář*: Conceptualization, Writing - Review & Editing

## 503 12. Colophon

504 This report was generated on 2022-05-30 15:14:38 using the following computational environment and  
505 dependencies:

```
506 #> - Session info -----  
507 #>   setting  value  
508 #>   version R version 4.2.0 (2022-04-22)  
509 #>   os        Manjaro Linux  
510 #>   system   x86_64, linux-gnu  
511 #>   ui        X11  
512 #>   language (EN)  
513 #>   collate   C  
514 #>   ctype     de_DE.UTF-8  
515 #>   tz        Europe/Zurich  
516 #>   date      2022-05-30  
517 #>   pandoc    2.17.1.1 @ /usr/bin/ (via rmarkdown)  
518 #>  
519 #> - Packages -----  
520 #>   package * version date (UTC) lib source  
521 #>   assertthat 0.2.1  2019-03-21 [1] CRAN (R 4.2.0)  
522 #>   bitops     1.0-7  2021-04-24 [1] CRAN (R 4.2.0)  
523 #>   bookdown   0.26   2022-04-15 [1] CRAN (R 4.2.0)  
524 #>   brio       1.1.3   2021-11-30 [1] CRAN (R 4.2.0)  
525 #>   cachem     1.0.6   2021-08-19 [1] CRAN (R 4.2.0)  
526 #>   callr      3.7.0   2021-04-20 [1] CRAN (R 4.2.0)  
527 #>   class      7.3-20  2022-01-16 [2] CRAN (R 4.2.0)  
528 #>   classInt   0.4-3   2020-04-07 [1] CRAN (R 4.2.0)  
529 #>   cli        3.3.0   2022-04-25 [1] CRAN (R 4.2.0)  
530 #>   colorspace 2.0-3   2022-02-21 [1] CRAN (R 4.2.0)  
531 #>   cowplot    * 1.1.1   2020-12-30 [1] CRAN (R 4.2.0)  
532 #>   crayon     1.5.1   2022-03-26 [1] CRAN (R 4.2.0)  
533 #>   curl       4.3.2   2021-06-23 [1] CRAN (R 4.2.0)  
534 #>   DBI        1.1.2   2021-12-20 [1] CRAN (R 4.2.0)  
535 #>   desc       1.4.1   2022-03-06 [1] CRAN (R 4.2.0)  
536 #>   devtools   2.4.3   2021-11-30 [1] CRAN (R 4.2.0)  
537 #>   digest     0.6.29  2021-12-01 [1] CRAN (R 4.2.0)  
538 #>   dplyr      1.0.9   2022-04-28 [1] CRAN (R 4.2.0)  
539 #>   e1071     1.7-9   2021-09-16 [1] CRAN (R 4.2.0)  
540 #>   ellipsis   0.3.2   2021-04-29 [1] CRAN (R 4.2.0)  
541 #>   evaluate   0.15    2022-02-18 [1] CRAN (R 4.2.0)  
542 #>   fansi      1.0.3   2022-03-24 [1] CRAN (R 4.2.0)  
543 #>   farver     2.1.0   2021-02-28 [1] CRAN (R 4.2.0)  
544 #>   fastmap    1.1.0   2021-01-25 [1] CRAN (R 4.2.0)  
545 #>   foreign    0.8-82  2022-01-16 [2] CRAN (R 4.2.0)
```

```

546 #> fs           1.5.2   2021-12-08 [1] CRAN (R 4.2.0)
547 #> generics     0.1.2   2022-01-31 [1] CRAN (R 4.2.0)
548 #> ggmap        * 3.0.0   2019-02-05 [1] CRAN (R 4.2.0)
549 #> ggplot2      * 3.3.6   2022-05-03 [1] CRAN (R 4.2.0)
550 #> ggrepel       * 0.9.1   2021-01-15 [1] CRAN (R 4.2.0)
551 #> ggsn         * 0.5.0   2019-02-18 [1] CRAN (R 4.2.0)
552 #> glue          1.6.2   2022-02-24 [1] CRAN (R 4.2.0)
553 #> gtable        0.3.0   2019-03-25 [1] CRAN (R 4.2.0)
554 #> here          * 1.0.1   2020-12-13 [1] CRAN (R 4.2.0)
555 #> highr         0.9     2021-04-16 [1] CRAN (R 4.2.0)
556 #> htmltools     0.5.2   2021-08-25 [1] CRAN (R 4.2.0)
557 #> httr          1.4.3   2022-05-04 [1] CRAN (R 4.2.0)
558 #> jpeg          0.1-9   2021-07-24 [1] CRAN (R 4.2.0)
559 #> KernSmooth    2.23-20  2021-05-03 [2] CRAN (R 4.2.0)
560 #> knitr         1.39    2022-04-26 [1] CRAN (R 4.2.0)
561 #> labeling       0.4.2   2020-10-20 [1] CRAN (R 4.2.0)
562 #> lattice        0.20-45  2021-09-22 [2] CRAN (R 4.2.0)
563 #> lifecycle      1.0.1   2021-09-24 [1] CRAN (R 4.2.0)
564 #> magrittr       2.0.3   2022-03-30 [1] CRAN (R 4.2.0)
565 #> maptools       1.1-4   2022-04-17 [1] CRAN (R 4.2.0)
566 #> memoise        2.0.1   2021-11-26 [1] CRAN (R 4.2.0)
567 #> munsell        0.5.0   2018-06-12 [1] CRAN (R 4.2.0)
568 #> pillar         1.7.0   2022-02-01 [1] CRAN (R 4.2.0)
569 #> pkgbuild       1.3.1   2021-12-20 [1] CRAN (R 4.2.0)
570 #> pkgconfig      2.0.3   2019-09-22 [1] CRAN (R 4.2.0)
571 #> pkgload         1.2.4   2021-11-30 [1] CRAN (R 4.2.0)
572 #> plyr          1.8.7   2022-03-24 [1] CRAN (R 4.2.0)
573 #> png            0.1-7   2013-12-03 [1] CRAN (R 4.2.0)
574 #> prettyunits    1.1.1   2020-01-24 [1] CRAN (R 4.2.0)
575 #> processx       3.5.3   2022-03-25 [1] CRAN (R 4.2.0)
576 #> proxy          0.4-26  2021-06-07 [1] CRAN (R 4.2.0)
577 #> ps              1.7.0   2022-04-23 [1] CRAN (R 4.2.0)
578 #> purrr          0.3.4   2020-04-17 [1] CRAN (R 4.2.0)
579 #> R6              2.5.1   2021-08-19 [1] CRAN (R 4.2.0)
580 #> RColorBrewer   1.1-3   2022-04-03 [1] CRAN (R 4.2.0)
581 #> Rcpp            1.0.8.3  2022-03-17 [1] CRAN (R 4.2.0)
582 #> remotes         2.4.2   2021-11-30 [1] CRAN (R 4.2.0)
583 #> rgdal           1.5-32  2022-05-09 [1] CRAN (R 4.2.0)
584 #> RgoogleMaps    1.4.5.3  2020-02-12 [1] CRAN (R 4.2.0)
585 #> rjson           0.2.21  2022-01-09 [1] CRAN (R 4.2.0)
586 #> rlang           1.0.2   2022-03-04 [1] CRAN (R 4.2.0)
587 #> rmarkdown        2.14    2022-04-25 [1] CRAN (R 4.2.0)
588 #> rnaturalearth  * 0.1.0   2017-03-21 [1] CRAN (R 4.2.0)
589 #> rprojroot       2.0.3   2022-04-02 [1] CRAN (R 4.2.0)
590 #> rstudioapi      0.13    2020-11-12 [1] CRAN (R 4.2.0)
591 #> s2              1.0.7   2021-09-28 [1] CRAN (R 4.2.0)
592 #> scales          1.2.0   2022-04-13 [1] CRAN (R 4.2.0)
593 #> sessioninfo     1.2.2   2021-12-06 [1] CRAN (R 4.2.0)
594 #> sf               * 1.0-7   2022-03-07 [1] CRAN (R 4.2.0)
595 #> sp               * 1.4-7   2022-04-20 [1] CRAN (R 4.2.0)
596 #> stringi          1.7.6   2021-11-29 [1] CRAN (R 4.2.0)
597 #> stringr          1.4.0   2019-02-10 [1] CRAN (R 4.2.0)
598 #> testthat         3.1.4   2022-04-26 [1] CRAN (R 4.2.0)
599 #> tibble          3.1.7   2022-05-03 [1] CRAN (R 4.2.0)

```

```
600 #> tidyverse      1.2.0  2022-02-01 [1] CRAN (R 4.2.0)
601 #> tidyselect     1.1.2  2022-02-21 [1] CRAN (R 4.2.0)
602 #> units          0.8-0  2022-02-05 [1] CRAN (R 4.2.0)
603 #> usethis        2.1.5  2021-12-09 [1] CRAN (R 4.2.0)
604 #> utf8           1.2.2  2021-07-24 [1] CRAN (R 4.2.0)
605 #> vctrs          0.4.1  2022-04-13 [1] CRAN (R 4.2.0)
606 #> withr          2.5.0  2022-03-03 [1] CRAN (R 4.2.0)
607 #> wk              0.6.0  2022-01-03 [1] CRAN (R 4.2.0)
608 #> xfun            0.31   2022-05-10 [1] CRAN (R 4.2.0)
609 #> yaml            2.3.5  2022-02-21 [1] CRAN (R 4.2.0)
610 #>
611 #> [1] /home/martin/R/x86_64-pc-linux-gnu-library/4.2
612 #> [2] /usr/lib/R/library
613 #>
614 #> -----
```